Soil Biology and Biochemistry 175 (2022) 108864

Contents lists available at ScienceDirect

Soil Biology and Biochemistry

journal homepage: www.elsevier.com/locate/soilbio

Long-term nitrogen enrichment accelerates soil respiration by boosting microbial biomass in coastal wetlands

Wendi Qu [a,b], Baohua Xie [b,c], Hao Hua [a,b], Gil Bohrer [d], Josep Penuelas [e,f], Chaoyang Wu [a,b,*], Guangxuan Han [b,c,**]

[a] The Key Laboratory of Land Surface Pattern and Simulation, Institute of Geographical Sciences and Natural Resources Research, Chinese Academy of Sciences, Beijing, 100101, China
[b] University of the Chinese Academy of Sciences, Beijing, 100049, China
[c] Key Laboratory of Coastal Zone Environmental Processes and Ecological Remediation, Yantai Institute of Coastal Zone Research, Chinese Academy of Sciences, Yantai, 264000, China
[d] Department of Civil, Environmental and Geodetic Engineering, The Ohio State University, Columbus, OH, USA
[e] CREAF, Centre de Recerca Ecològica i Aplicacions Forestals, Cerdanyola del Vallès, Barcelona, 08193, Catalonia, Spain
[f] CSIC, Global Ecology Unit CREAF-CSIC-UAB, Bellaterra, Barcelona, 08193, Catalonia, Spain

ARTICLE INFO

Keywords:
Nitrogen enrichment
Coastal wetlands
Soil respiration
Microbial biomass carbon
Temperature sensitivity

ABSTRACT

Coastal wetlands are essential in terrestrial carbon balance because they act as natural "blue carbon" sinks, influenced by anthropogenic nitrogen (N) enrichment. N enrichment alters soil environment and plant growth, impacting carbon loss through soil respiration (R_{soil}). However, the responses of R_{soil} to N enrichment remain elusive in coastal wetlands, hindering the estimation of carbon fluxes. To bridge this knowledge gap, we used an 8-year field N fertilization platform in the coastal wetlands of the Yellow River Delta, China, to measure R_{soil} composed of heterotrophic respiration and autotrophic respiration, and multiple indicators of soil properties, microbial activities, and plant growth. We found long-term N enrichment increased Rsoil by 26.6 ± 1.2% (mean ± standard deviation) and quadrupled microbial biomass carbon, accounting for 26.9 ± 1.2% of the increase in heterotrophic respiration. In addition, N enrichment boosted plant growth, increasing the above-ground biomass by 28.7 ± 6.9% while inducing a cooling effect that partly offsets the increase in autotrophic respiration. In particular, N enrichment elevated soil temperature sensitivity of Rsoil with the increase of N levels, suggesting that the nutrient-related control of Rsoil responds to warming. The study indicates that N enrichment stimulates R_{soil} in coastal wetlands by boosting microbial biomass carbon through interactions between soil environmental conditions and plant growth. These results have implications for predicting the carbon cycle with anthropogenic N enrichment.

1. Introduction

Coastal wetlands are productive ecosystems with a slow decomposition rate of soil organic carbon, acting as "blue carbon" sinks and are one of the natural climate solutions (Krauss et al., 2018; Macreadie et al., 2021; Wang et al., 2021). Climate warming, hydrological events (e.g., flooding), and anthropogenic activities (e.g., agricultural fertilization) alter the structure and function of coastal wetlands, impacting ecosystem energy flowing and biogeochemical cycle (Han et al., 2015; Millennium Ecosystem Assessment, 2005). The response of carbon dynamics to environmental change in coastal wetlands depends on plant community composition, soil salinity, and local nutrient stress, such as the conditions of nitrogen (N) deposition (Caplan et al., 2015). Changes in N availability can alter the ecosystem productivity via photosynthesis and soil carbon loss via soil respiration (R_{soil}), further regulating the resilience of coastal wetlands and ecosystem services.

Anthropogenic N enrichment of ecosystems, primarily through fuel combustion and agricultural fertilization, regulates ecosystem carbon

* Corresponding author. The Key Laboratory of Land Surface Pattern and Simulation, Institute of Geographical Sciences and Natural Resources Research, Chinese Academy of Sciences, Beijing, 100101, China.
** Corresponding author. Key Laboratory of Coastal Zone Environmental Processes and Ecological Remediation, Yantai Institute of Coastal Zone Research, Chinese Academy of Sciences, Yantai, 264000, China.
E-mail addresses: wucy@igsnrr.ac.cn (C. Wu), gxhan@yic.ac.cn (G. Han).

https://doi.org/10.1016/j.soilbio.2022.108864
Received 16 August 2022; Received in revised form 14 October 2022; Accepted 20 October 2022
Available online 23 October 2022

cycling (Liu and Greaver, 2010; Wilcots et al., 2022). Increased N availability stimulates plant growth and nutrient enhancement in plant tissue, improving plant carbon uptake ("carbon sink"), especially in N-limited regions (Galloway et al., 2008; Liu et al., 2013). N enrichment could either accelerate or limit soil carbon loss by increasing or reducing R_{soil} and dissolved organic carbon leaching ("carbon source"), respectively (Bragazza et al., 2006; Liu and Greaver, 2009). In coastal wetlands, the alleviation of N constraints on microbial metabolism, the amelioration of litter quality, and enhanced enzymatic activity may account for the stimulating effects of N enhancement on R_{soil} (Tao et al., 2018; Wang et al., 2019; Wolters et al., 2016). For example, N input in saline-alkaline soil of coastal wetlands could elevate soil carbon storage with higher plant biomass and more favorable soil environment, proliferating the diffusion of substrates for soil microbes and accelerating R_{soil} (Qu et al., 2019). However, as one of the main consequences of N enrichment, soil acidification increases the concentration of Al^{3+} in the porewater, strengthening environmental stress on plant roots and soil microbes (Meng et al., 2019; Tian and Niu, 2015). For example, additional N input in N-abundant forests and croplands reduces below-ground carbon allocation and deteriorates the soil environment (e.g., soil pH stress), depressing soil microbial activities and inhibiting R_{soil} (Fu et al., 2020; Mo et al., 2008; Wang et al., 2018). So far, the physiochemical impacts of N enrichment on R_{soil} and underlying mechanisms are elusive in coastal wetlands, hindering our knowledge of ecosystem carbon balance and climate feedback.

The two components of R_{soil} are autotrophic respiration (R_a) and heterotrophic respiration (R_h). Their patterns in response to N enrichment may be inconsistent (Liu and Greaver, 2010), because plant roots and soil microbes react differently to environmental changes. A meta-analysis reported that additional N input raises N content in roots by 27.6%, further boosting root production by 23% and enormously increasing the rate of R_a (Xia and Wan, 2008). However, N enrichment could decrease the size of microbial populations (Liu and Greaver, 2010) and depress the activity of lignolytic enzymes of litter-decomposing fungi, further limiting R_h under N enrichment (Pregitzer et al., 2008; Zak et al., 2008). The inconsistent effects of N enrichment on R_{soil} in different ecosystems could be associated with the divergent responses of R_a and R_h to N enrichment (Greaver et al., 2016; Liu and Greaver, 2010). Few studies have focused on the relative impacts of N enrichment on R_a and R_h and their associated drivers in coastal wetlands. Unlike other N-limited ecosystems, tidal coastal wetlands are characterized by high soil salinity and alkalinity. Thus, the impacts of N enrichment on the soil environment and microbial activities in coastal wetlands could be greatly different from or opposite to the effect in other N-limited ecosystems (Min et al., 2011). Therefore, a comprehensive investigation of N enrichment effects on R_{soil} integrating soil environment, plant growth, and microbial activities is needed to accurately predict "blue carbon" sinks in coastal wetlands, which are experiencing, or facing in the near future, increasing N deposition.

Soil microbial respiration is highly sensitive to temperature, indicating the temperature sensitivities of microbial growth and metabolism (e.g., enzyme activities and C use efficiency) (Li et al., 2020). Soil temperature sensitivity (Q_{10}), defined as the factor by which the R_{soil} rate increases by a 10 °C increase in temperature, is substantially controlled by soil N availability (Eberwein et al., 2015; Zhang et al., 2014). However, a quantitative response of Q_{10} to N enrichment with different levels is lacking in coastal wetlands. To this end, we conducted long-term *in situ* experiments consisting of 8-year N enrichment in the coastal wetlands of the Yellow River Delta (YRD), China, followed by a one-year field measurements campaign at the experimental site. We measured R_{soil} and distinguished its components, R_a and R_h, soil physiochemical properties, plant growth, microbial biomass, and microbial community structure. The goal of the study was threefold: first, to analyze the impacts of long-term N enrichment on R_{soil} and associated biotic and abiotic factors; second, to investigate the response of Q_{10} to varied levels of N enrichment in coastal wetlands; third, to improve the understanding of the underlying mechanisms through which N enrichment affected soil carbon dynamics.

2. Materials and methods

2.1. Site description and field N fertilization experiment

This experiment began in 2012 and was conducted in the Yellow River Delta (YRD) Ecological Research Station of Coastal Wetlands, Chinese Academy of Sciences (37°36′N, 118°57′E). The YRD coastal wetlands are one of the most widely preserved and youngest wetland ecosystems in the warm temperate zones of the world. The local atmospheric N deposition rate is nearly 2.1 g N m^{-2} $year^{-1}$ during the growing season (Guan et al., 2019). Variable groundwater level (from 1 m to 3 m) was reported due to land-ocean interactions and abundant precipitation during the growing season (Han et al., 2015). This area has extensive saline-alkaline soil because of high evaporation (Qu et al., 2019). The YRD coastal wetlands are warm and semi-humid, with an annual average temperature of 13 °C, fluctuating between a cold winter (average temp. −2.8 °C) and a warm summer (26.7 °C) and a total rainfall of 560 mm per year, peaking in July–August (Han et al., 2018). *Phragmites australis* and *Suaeda salsa* are the two dominant herbaceous species, with an average canopy height of 1.7 m and a closure vegetation index of 0.8 (Han et al., 2015). In the experiment area, the dominant plant is *Phragmites australis*.

We set up 20 experimental plots (4 levels x 5 replicates, 4 m × 6 m each) sparsely distributed in a large experiment field (50 plots in total) to avoid potential N movement and loss (Fig. 1). We designed four levels of N fertilization rates, i.e., 0 g N m^{-2} yr^{-1} (or control ground, N0), 5 g N m^{-2} yr^{-1} (N5), 10 g N m^{-2} yr^{-1} (N10), and 20 g N m^{-2} yr^{-1} (N20). These fertilization rates were chosen to simulate normal to severe levels of anthropogenic atmospheric N deposition (Guan et al., 2019; Wilcots et al., 2022). Each treatment was replicated five times to reduce potential uncertainty. We applied N in the form of ammonium nitrate (NH_4NO_3), which is a common fertilizer. Fertilizer was applied in the treatment plots once per month from 01/2012 to now, which we dissolved in 1.2 L deionized water and sprayed it over each plot evenly. We sprayed deionized water without fertilizer in the N0 control plots to keep soil water content unbiased. To avoid the interception of fertilizer by plants, we sprayed fertilizer directly onto the soil or plant root.

2.2. Soil respiration measurements

After 8 years of continuous N enrichment, we started biweekly respiration measurements (from 202001-01 to 2020-12-15). To better disentangle R_a and R_h from R_{soil}, we installed the polyvinyl chloride polymer collars two years earlier than the respiration measurements in each plot (Sun et al., 2020). Specifically, we installed two polyvinyl chloride polymer collars with a radius of 21 cm in the soil at the center of each plot: one was 5 cm deep for R_{soil} measurements, and the other was 40 cm deep for R_h measurements. Respiration (CO_2 flux) was measured by an LGR Ultraportable Greenhouse Gas Analyzer (UGGA, Los Gatos Research, Inc., San Jose, USA) that measures gas concentrations continuously (at a frequency of 1 Hz) in a chamber placed over the collar. The chamber was transparent and made of plexiglass with a radius of 40 cm. To remove plant respiration above the ground, we carefully clipped living plants inside the collars one day before each measurement. At each plot, R_{soil} was continuously measured from 08:00 to 12:00 (noon) in local time to minimize the effects of diurnal variations.

2.3. Measurements of soil and plant indicators

We sampled and measured total plant biomass in October 2020 (at the end of the growing season). To do so, we first selected five small quadrats (1 m × 1 m) by randomly in each experimental plot (4 m × 6

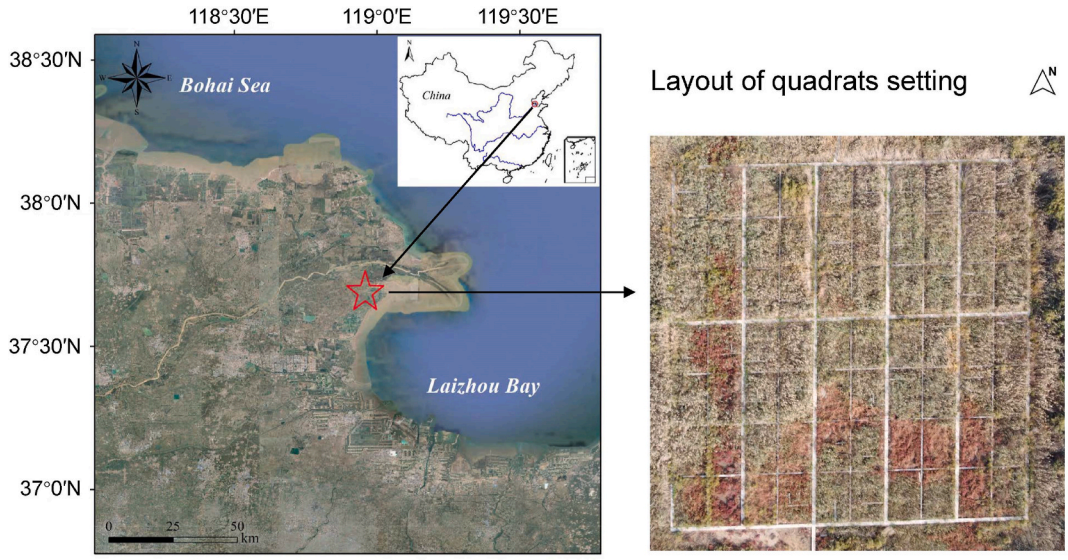

Fig. 1. Location of the study site. The right layout is a bird-view image of the experimental field derived from an unmanned aerial vehicle.

m) and sampled all plants and soil (0–10 cm) in each quadrat. Total plant biomass was calculated as the sum of plant biomass above the ground and below the ground. Then, we put the plant samples in rigid envelopes and dried them in the oven (80 °C) for two days to measure the biomass (g m^{-2}). Regarding soil properties, the extractable N is the total amount of NH_4^+-N and NO_3^--N in soil samples. We used three-parameter sensors to measure the top-layer (0–10 cm) soil temperature (ST, °C), soil moisture (SM, %), and soil electrical conductivity (ds cm^{-1}).

2.4. Soil microbe analyses

We sampled the fresh soil at the peak of the growing season in July 2020. To estimate the microbial population, we measured the microbial biomass carbon using a Shimadzu TOC analyzer (TOC-VCPH) and the chloroform-fumigation extraction method (Brookes et al., 1985). To analyze the microbial community structure, we first extracted total DNA using a PowerSoil DNA Isolation Kit (MO BIO Laboratories, Inc., USA) and preserved the samples at −20 °C. The primers 341F and 806R were applied to target the bacterial 16S rRNA gene in V3–V4 fragments and identify functional microorganisms (Mori et al., 2014). We then carried out the reactions (50 μl in total) using 25 μl of 2 × Primer Taq (TaKaRa, RR902A), 1 μl forward primer (10 mM), 1 μl of reverse primer (10 mM), 3 μl of g-DNA, and 20 μl of nuclease-free water.

The thermal cycling was conducted as follows: (1) 94 °C for 5 min, (2) 31 cycles of 94 °C for 30 s, (3) 52 °C for 30 s, (4) 72 °C for 45 s, (5) 72 °C for 10 min, and (6) held at 72 °C before purification (Xu et al., 2016). The gel electrophoresis was used to analyze the PCR products. Pyrosequencing was performed on the MiSeq platform. We used Trimmomatic-0.33 for data quality control and the filtration of the raw sequence reads. Afterwards, we removed the reads identified as putative chimaeras by the MOTHUR project (Li et al., 2022). To quantify the degree of similarity between the sequences, we defined a threshold (≥97%) to derive the operational taxonomic units (OTUs) at the species level (Gu et al., 2019; Xu et al., 2016). We completed the taxonomic assignments using the UCLUST method with a similarity of 0.5. Finally, we obtained reference sequences from the Greengenes OTU database (gg_13_8_otus, http://qiime.org/home_static/dataFiles.html).

2.5. Statistical analysis

We conducted the one-way analyses of variance (ANOVA) in IBM SPSS Statistics given that only N level is different in our experiment. The differences were significant when the p-value was lower than 0.05. Pearson correlation analyses were used to determine the correlations between R_{soil} and N-related biotic and abiotic factors. To investigate the impact of above-ground biomass on ST, we also used partial correlation analyses to exclude the effects of other potential factors (i.e., SM, electrical conductivity, and extractable N). Moreover, principal coordinate analyses (PCoA) were used to check the differences between treatments in soil microbial community structure using the 'Vegan' package in R (v.4.1.1). We also used the analysis of similarities (ANOSIM) based on Bray-Curtis distance for the significant difference tests of the microbial community structure.

We applied structural equation modeling (SEM) to quantitatively describe direct and indirect relationships between N enrichment and R_{soil}. We assumed that N enrichment boosts R_{soil} through impacting microbial activities, plant growth, and soil environment. For the evaluation of the SEM fit, we calculated the standardized root mean square residual, the chi-square to degrees of freedom ratio, and the normed fit index (Hair et al., 2017). Given the small sample size (<100), we applied the partial least square (PLS) method to simulate a complex predictive path (Wong, 2013). The SEM analyses were carried out using the 'Lavaan' package in R (v.4.1.1) (Rosseel, 2012).

3. Results

3.1. Impacts of N enrichment on R_{soil}, soil properties, and plant growth

Long-term N enrichment stimulated R_{soil}, R_h, and R_a with average enhancements of 26.6%, 26.9%, and 26.4% compared to N0, respectively ($p < 0.05$). When comparing N5, N10, and N20, no significant differences were found (Fig. 2a–c). N enrichment had a significant effect on soil temperature and electrical conductivity ($p < 0.05$), with an average decline of 13.1% and 24.6%, respectively (Fig. 2f). Regarding plant growth, N enrichment increased above-ground biomass by 28.7% ($p < 0.05$), with no significant effect on below-ground biomass (Fig. 2g–h).

3.2. Responses of soil microbial biomass and community structure to N enrichment

Compared to the N0 group, N enrichment significantly increased microbial biomass carbon by 436.2% on average ($p < 0.001$), and the highest microbial biomass carbon (306 μg g^{-1}) was observed in the N20 group (Fig. 3a). High-throughput sequencing analysis of the 20 samples

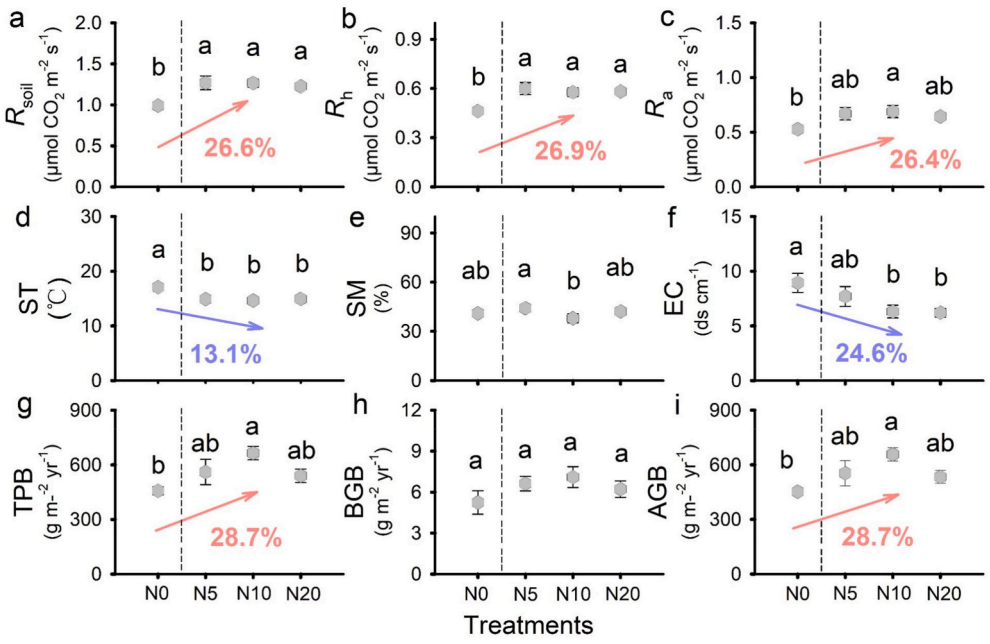

Fig. 2. Effects of N enrichment on soil respiration, soil properties, and plant biomass. Subfigures a-i show the distributions of soil respiration (R_{soil}), heterotrophic respiration (R_h), autotrophic respiration (R_a), soil temperature (ST), soil moisture (SM), electrical conductivity (EC), total plant biomass (TPB), below-ground biomass (BGB), and above-ground biomass (AGB) (mean ± standard deviation). Different lowercase letters indicate a statistically significant difference ($p < 0.05$). N0, N5, N10, and N20 represent the N enrichment treatments with 0, 5, 10 and 20 g N m^{-2} yr^{-1}, respectively. Arrows with labels indicate the average increases (red) or decreases (blue) in variables (%). (For interpretation of the references to color in this figure legend, the reader is referred to the Web version of this article.)

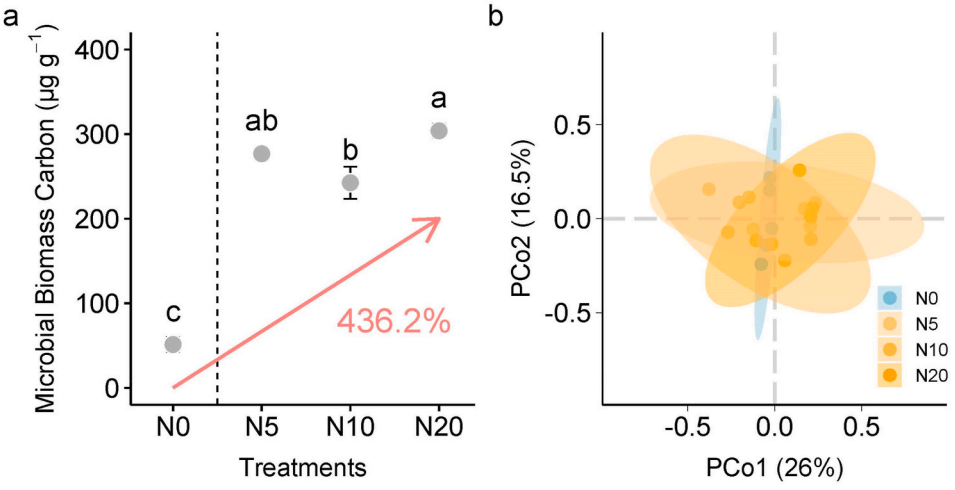

Fig. 3. Impacts of N enrichment on microbial biomass carbon and microbial community structure. (a) Distribution of microbial biomass carbon under N enrichment. Different lower-case letters indicate a significant difference ($p < 0.05$). Arrow with label indicates the average increases (red) in microbial biomass carbon (%). (b) Principal coordinate analyses (PCoA) plot of soil microbial community structure between N enrichment treatments. N0, N5, N10, and N20 represent the N enrichment treatments with 0, 5, 10 and 20 g N m^{-2} yr^{-1}, respectively. (For interpretation of the references to color in this figure legend, the reader is referred to the Web version of this article.)

yielded 45212 valid reads to facilitate the beta-diversity analyses of microbial communities under N enrichment treatments. We found no appreciable differences in the microbial community structures. PCoA of microbial communities (Fig. 3b) failed to separate the groups of soils under the four treatment regimens. Dissimilarity analyses found no statistically significant difference in bacterial community structure under N-added treatments and non-N control (Table 1).

Table 1
Dissimilarity test of bacterial community structure under N enrichment on the basis of Bray-Curtis distance. The values of the upper triangular matrices (highlighted in bold) are the statistically significance value (p). The values of the lower triangular matrices are the analysis of similarities (ANOSIM) r statistic. N0, N5, N10, and N20 represent the N enrichment treatments with 0, 5, 10 and 20 g N m^{-2} yr^{-1}, respectively.

Treatments	ANOSIM			
	N0	N5	N10	N20
N0	0	**0.318**	**0.8**	**0.42**
N5	0.012	0	**0.612**	**1**
N10	−0.116	−0.08	0	**0.648**
N20	−0.024	−0.208	−0.068	0

3.3. Impacts of N enrichment on soil temperature sensitivity

R_{soil} showed exponential increases along the soil temperature gradients under N enrichment ($p < 0.001$) (Fig. 4a–d). Compared to the N0 group with a Q_{10} of 2.175, N enrichment overall enhanced Q_{10} for all N treatments ($p > 0.05$, Fig. 4e). This enhancement was positively correlated with the N enrichment levels, ranging from 2.226 to 2.298. Significant difference in base soil respiration was observed between non-added and N-added groups ($p < 0.05$, Fig. 4f).

3.4. Mechanisms of the impacts of N enrichment on R_{soil}

R_{soil} was significantly and positively correlated with microbial biomass carbon ($r = 0.62$, $p < 0.01$). Similar effects of microbial biomass carbon and below-ground biomass on R_h and R_a were observed. Interestingly, we found ST was negatively correlated with R_{soil}, R_h, microbial biomass carbon, and above-ground biomass ($p < 0.05$) (Fig. 5a). After

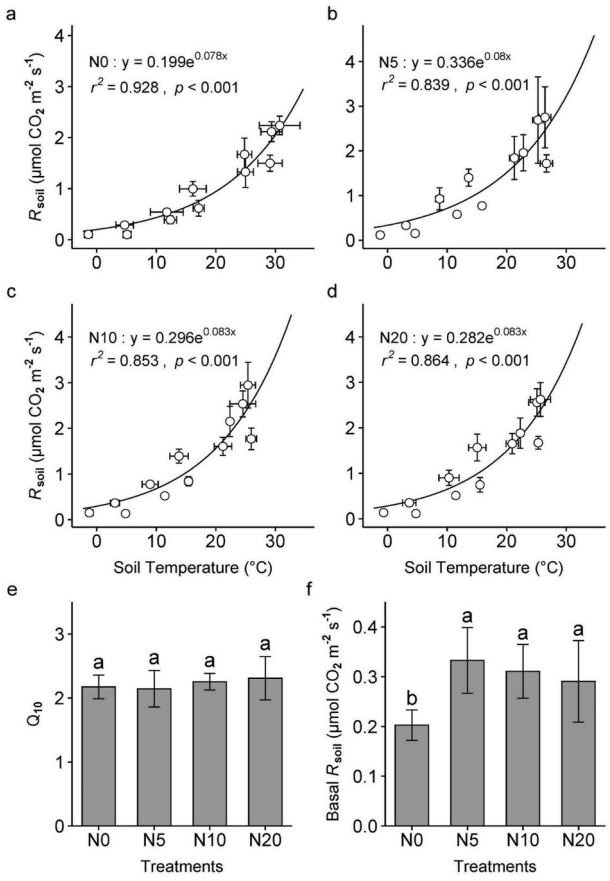

Fig. 4. Relationships between soil respiration (R_{soil}) and soil temperature under N enrichment. N0, N5, N10, and N20 represent the N enrichment treatments with 0, 5, 10 and 20 g N m^{-2} yr^{-1}, respectively. Q_{10} indicates the factor by which the R_{soil} rate would increase following a 10 °C increase in temperature. Different lower-case letters indicate a significant difference ($p < 0.05$).

removing the effects of SM, electric conductivity, and extractable N, a partial correlation analysis also showed that ST was negatively correlated with above-ground biomass (r = −0.48, $p < 0.05$) (Fig. 5b).

The significance criteria of SEM model fitting were satisfied with a goodness of fit index of 1.0. The fitted model explained 83.7% of the variance of R_{soil}, 32.9% of the variance of the microbe, 16.4% of the variance of vegetation, 25.5% of the variance of electric conductivity, and 27% of the variance of ST, respectively (Fig. 6). Long-term N enrichment enhanced microbial biomass carbon and further boosted R_h, with a stimulating effect on R_{soil} ($p < 0.001$). Interestingly, below-ground biomass positively impacted R_{soil} through R_a, while the above-ground biomass had a direct and negative influence on ST ($p < 0.001$) and indirectly reduced R_{soil}.

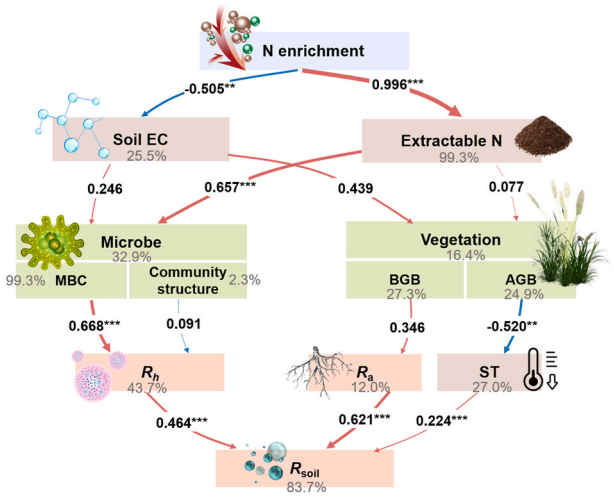

Fig. 6. Structural equation model (SEM) analysis describing the impacts of N enrichment on soil respiration (R_{soil}). EC, soil electric conductivity; MBC, microbial biomass carbon; BGB, below-ground biomass; AGB, above-ground biomass; ST, soil temperature; R_h, soil heterotrophic respiration; and R_a, soil autotrophic respiration. Red and blue arrows indicate positive and negative effects, respectively. The width of the arrow lines is proportional to the strength of the corresponding relationship. The numbers adjacent to the arrows are standardized path coefficients. The percentages in grey next to variables refer to the variance explained by the model. Significant correlations were marked with * ($p < 0.05$), ** ($p < 0.01$), and *** ($p < 0.001$) (n = 20). (For interpretation of the references to color in this figure legend, the reader is referred to the Web version of this article.)

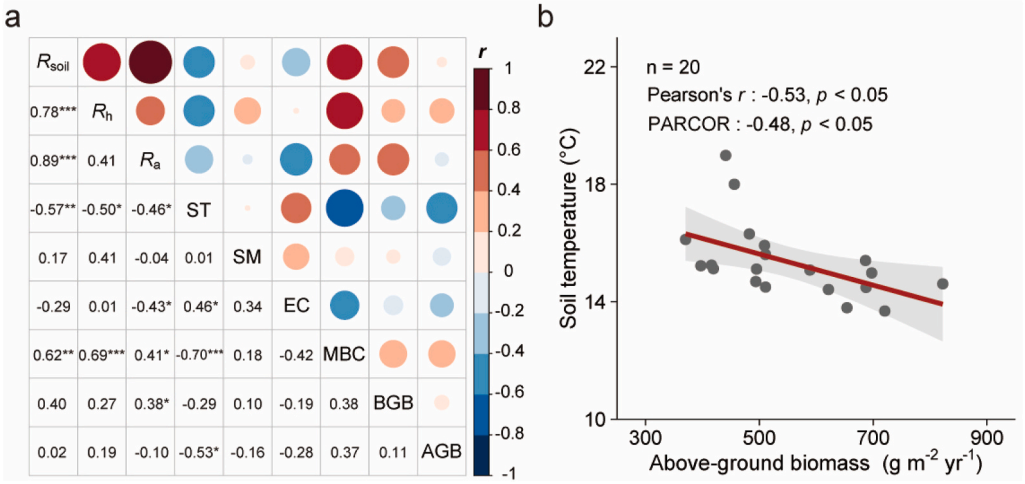

Fig. 5. Pair-wise Pearson correlation coefficients between indicators of soil respiration (R_{soil}), soil environment, soil microbes, and plant growth. (a) Pearson correlation coefficients among R_{soil}, heterotrophic respiration (R_h), autotrophic respiration (R_a), soil temperature (ST), soil moisture (SM), electric conductivity (EC), microbial biomass carbon (MBC), below-ground biomass (BGB), and above-ground biomass (AGB). Significant correlations were marked with * ($p < 0.05$), ** ($p < 0.01$), and *** ($p < 0.001$) (n = 20). The size and color of circles at the upper triangular correspond to the correlation coefficients in the squares in the bottom left. (b) Relationship between soil temperature and above-ground biomass. PARCOR indicates the partial correlation coefficient between ST and above-ground biomass, controlling the effects of SM, electric conductivity, and soil extractable N. (For interpretation of the references to color in this figure legend, the reader is referred to the Web version of this article.)

4. Discussion

4.1. N enrichment regulates R_{soil} through soil environment and plant growth

Plant growth and soil physiochemical characteristics are directly affected by N addition (Janssens et al., 2010; Wilcots et al., 2022). Given that the coastal wetlands of YRD are N-limited, N addition alleviated nutrient stress and boosted plant growth with enhanced plant biomass (Fig. 2h and j). We found that there was a significant decrease (−24.6%, $p < 0.05$) in soil electric conductivity under N enrichment (Fig. 2f), and that lower electric conductivity benefited both the microbial biomass and plant growth, accelerating carbon fluxes through R_{soil} and photosynthesis, respectively (Fig. 6). We thus provide the potential mechanism that links N enrichment and variations in plant growth, soil temperature, and electric conductivity. The unexpectedly adverse effects of N enrichment on soil temperature could be associated with the increase in above-ground biomass. Enhanced above-ground biomass is characterized by a higher leaf area index, and thus more shading of the soil that leads to a cooling effect on the soil beneath the plant, lowering potential evaporation and electrical conductivity accordingly (Qu et al., 2019; Shaygan et al., 2018). After we excluded possible effects of SM, electrical conductivity, and available N, the partial correlation analysis confirmed the negative correlation between above-ground biomass and soil temperature (Fig. 5b), suggesting a negative vegetation-mediated feedback between N enrichment and R_{soil} through soil cooling (Piao et al., 2020).

4.2. N enrichment enhances R_{soil} through boosting microbial biomass carbon instead of altering community structure

Long-term N addition could weaken soil microbial activity through acidification and osmotic pressure from the oxidation of NH_4^+ to NO_3^- (Janssens et al., 2010; Qu et al., 2019; Tian and Niu, 2015). However, we observed an obvious increase in both microbial biomass carbon (+436.2%) and the rate of R_h under N enrichment (Fig. 3a), which can be mainly explained by the accumulation of soil nutrients (i.e., extractable N) (Fig. 6). Moreover, plant growth under N enrichment increased soil carbon content, further benefiting microbial metabolism and reproduction (Qu et al., 2019).

Numerous studies investigated the role of N enrichment in microbial community structure and functions (Frey et al., 2004; Liu et al., 2020). For example, it has been reported that farmyard manure applications with N fertilizer accelerate soil carbon cycling through boosting microbial biomass carbon instead of altering microbial community structure (Ma et al., 2020). Similarly, when using both PCoA and ANOSIM, we found that long-term N enrichment in coastal wetlands generated no noticeable change in the microbial community structure (Fig. 3b and Table 1). Unlike other ecosystems (e.g., forests and grasslands with high microbial biodiversity), the coastal wetlands of YRD under tidal erosion are abundant with salt-tolerant microbes (Li et al., 2022), to some degree fixing the diversity of microbes under N enrichment. Thus, the stimulating effects of N enrichment on R_h in YRD were mainly controlled by microbial community population size (microbial biomass carbon) instead of its structure.

4.3. Potential impact of N enrichment on soil carbon dynamics in coastal wetlands

The temperature sensitivity of R_{soil} (i.e., Q_{10}) is a key parameter used for modeling carbon dynamics. Q_{10} varies with environmental soil types and conditions. Similar to stimulating impacts of N enrichment on R_{soil}, we observed increases in Q_{10} (ranging from +3% to +7%) along the increase of N enrichment, suggesting an N-dependent response of R_{soil} to temperature in coastal wetlands (Fig. 4). Mo et al. (2008) reported that excessive N addition reduced Q_{10} in N-rich forests and lowered R_{soil}, possibly because of the soil C:N ratio threshold. In contrast, in the N-limited coastal wetlands of YRD, N enrichment caused simultaneous enhancement of N availability and Q_{10}.

Considering the cooling effect of above-ground biomass, we proposed that N-added plant growth partly offset the stimulating impacts on R_{soil} by lowering the soil temperature coupled with higher Q_{10}. Wetlands' greening has been reported from field and satellite observations (Zhu et al., 2016). Wetlands greening may benefit local ecosystem carbon sequestration in two ways. First, increasing greenness is associated with higher productivity, and plants can uptake and fix more carbon through photosynthesis. Second, more vegetation cover could lower ST, especially during daytime, which leads to less carbon released from soil to the atmosphere.

5. Conclusions

Coastal wetlands play an essential role in global carbon sequestration, but the potential drivers of soil carbon dynamics remain elusive. Here we investigated the impact of long-term N enrichment on soil carbon release (i.e., R_{soil}) and underlying mechanisms in the Yellow River Delta coastal wetlands, China. We found that long-term N enrichment accelerated soil carbon loss via R_{soil}, by interactions between soil environment, microbial activities, and plant growth. Specifically, increased N availability boosted microbial activities and, accordingly, the rate of R_{soil} via increasing microbial biomass instead of changing its community structure. Our results highlight the importance of N cycling, especially anthropogenic N enrichment, in current soil carbon dynamics and future projections in coastal wetlands. The impact of N deposition on vegetation dynamics, soil carbon release, and their interactions, especially on a large scale (at the ecosystem or global level), could have a significant effect on the global carbon budget. These effects are complex and further investigations are needed for improved carbon budget prediction by ecosystem models.

Declaration of competing interest

The authors declare that they have no known competing financial interests or personal relationships that could have appeared to influence the work reported in this paper.

Data availability

I have shared the link to my data in the manuscript.

Acknowledgements

This research was supported by the Natural Science Foundation of China (U2106209, 42071126, 42101117), the Strategic Priority Research Program of the Chinese Academy of Sciences (XDA23050202), and the International Science Partnership Program of the Chinese Academy of Sciences (121311KYSB20190029).

References

Bragazza, L., Freeman, C., Jones, T., Rydin, H., Limpens, J., Fenner, N., Ellis, T., Gerdol, R., Hájek, M., Hájek, T., Iacumin, P., Kutnar, L., Tahvanainen, T., Toberman, H., 2006. Atmospheric nitrogen deposition promotes carbon loss from peat bogs. Proceedings of the National Academy of Sciences (USA) 103, 19386–19389. https://doi.org/10.1073/pnas.0606629104.

Brookes, P.C., Kragt, J.F., Powlson, D.S., Jenkinson, D.S., 1985. Chloroform fumigation and the release of soil nitrogen: the effects of fumigation time and temperature. Soil Biology and Biochemistry 17, 831–835. https://doi.org/10.1016/0038-0717(85)90143-9.

Caplan, J.S., Hager, R.N., Megonigal, J.P., Mozdzer, T.J., 2015. Global change accelerates carbon assimilation by a wetland ecosystem engineer. Environmental Research Letters 10. https://doi.org/10.1088/1748-9326/10/11/115006.

Eberwein, J.R., Oikawa, P.Y., Allsman, L.A., Jenerette, G.D., 2015. Carbon availability regulates soil respiration response to nitrogen and temperature. Soil Biology and Biochemistry 88, 158–164. https://doi.org/10.1016/j.soilbio.2015.05.014.

Frey, S.D., Knorr, M., Parrent, J.L., Simpson, R.T., 2004. Chronic nitrogen enrichment affects the structure and function of the soil microbial community in temperate hardwood and pine forests. Forest Ecology and Management 196, 159–171. https://doi.org/10.1016/j.foreco.2004.03.018.

Fu, W., Wu, H., Zhao, A.H., Hao, Z.P., Chen, B.D., 2020. Ecological impacts of nitrogen deposition on terrestrial ecosystems: research progresses and prospects. Chinese Journal of Plant Ecology 44, 475–493. https://doi.org/10.17521/CJPE.2019.0163.

Galloway, J.N., Townsend, A.R., Erisman, J.W., Bekunda, M., Cai, Z., Freney, J.R., Martinelli, L.A., Seitzinger, S.P., Sutton, M.A., 2008. Transformation of the nitrogen cycle: recent trends, questions, and potential solutions. Science 320, 889–892. https://doi.org/10.1126/science.1136674.

Greaver, T.L., Clark, C.M., Compton, J.E., Vallano, D., Talhelm, A.F., Weaver, C.P., Band, L.E., Baron, J.S., Davidson, E.A., Tague, C.L., Felker-Quinn, E., Lynch, J.A., Herrick, J.D., Liu, L., Goodale, C.L., Novak, K.J., Haeuber, R.A., 2016. Key ecological responses to nitrogen are altered by climate change. Nature Climate Change 6, 836–843. https://doi.org/10.1038/nclimate3088.

Gu, S., Hu, Q., Cheng, Y., Bai, L., Liu, Z., Xiao, W., Gong, Z., Wu, Y., Feng, K., Deng, Y., Tan, L., 2019. Application of organic fertilizer improves microbial community diversity and alters microbial network structure in tea (Camellia sinensis) plantation soils. Soil and Tillage Research 195, 104356. https://doi.org/10.1016/j.still.2019.104356.

Guan, B., Xie, B., Yang, S., Hou, A., Chen, M., Han, G., 2019. Effects of five years' nitrogen deposition on soil properties and plant growth in a salinized reed wetland of the Yellow River Delta. Ecological Engineering 136, 160–166. https://doi.org/10.1016/j.ecoleng.2019.06.016.

Hair, J., Hollingsworth, C.L., Randolph, A.B., Chong, A.Y.L., 2017. An updated and expanded assessment of PLS-SEM in information systems research. Industrial Management & Data Systems 117, 442–458. https://doi.org/10.1108/IMDS-04-2016-0130.

Han, G., Chu, X., Xing, Q., Li, D., Yu, J., Luo, Y., Wang, G., Mao, P., Rafique, R., 2015. Effects of episodic flooding on the net ecosystem CO_2 exchange of a supratidal wetland in the Yellow River Delta. Journal of Geophysical Research: Biogeosciences 120, 1506–1520. https://doi.org/10.1002/2015JG002923.

Han, G., Sun, B., Chu, X., Xing, Q., Song, W., Xia, J., 2018. Precipitation events reduce soil respiration in a coastal wetland based on four-year continuous field measurements. Agricultural and Forest Meteorology 256 (257), 292–303. https://doi.org/10.1016/j.agrformet.2018.03.018.

Janssens, I.A., Dieleman, W., Luyssaert, S., Subke, J.-A., Reichstein, M., Ceulemans, R., Ciais, P., Dolman, A.J., Grace, J., Matteucci, G., Papale, D., Piao, S.L., Schulze, E.-D., Tang, J., Law, B.E., 2010. Reduction of forest soil respiration in response to nitrogen deposition. Nature Geoscience 3, 315–322. https://doi.org/10.1038/ngeo844.

Krauss, K.W., Noe, G.B., Duberstein, J.A., Conner, W.H., Stagg, C.L., Cormier, N., Jones, M.C., Bernhardt, C.E., Graeme Lockaby, B., From, A.S., Doyle, T.W., Day, R. H., Ensign, S.H., Pierfelice, K.N., Hupp, C.R., Chow, A.T., Whitbeck, J.L., 2018. The role of the upper tidal estuary in wetland blue carbon storage and flux. Global Biogeochemical Cycles 32, 817–839. https://doi.org/10.1029/2018GB005897.

Li, J., Han, G., Wang, G., Liu, X., Zhang, Q., Chen, Y., Song, W., Qu, W., Chu, X., Li, P., 2022. Imbalanced nitrogen–phosphorus input alters soil organic carbon storage and mineralisation in a salt marsh. Catena 208, 105720. https://doi.org/10.1016/j.catena.2021.105720.

Li, J., Pei, J., Pendalls, E., Fang, C., Nie, M., 2020. Spatial heterogeneity of temperature sensitivity of soil respiration: a global analysis of field observations. Soil Biology and Biochemistry 141, 107675.

Liu, L., Greaver, T.L., 2010. A global perspective on belowground carbon dynamics under nitrogen enrichment. Ecology Letters 13, 819–828. https://doi.org/10.1111/j.1461-0248.2010.01482.x.

Liu, L., Greaver, T.L., 2009. A review of nitrogen enrichment effects on three biogenic GHGs: the CO_2 sink may be largely offset by stimulated N_2O and CH_4 emission. Ecology Letters 12, 1103–1117. https://doi.org/10.1111/j.1461-0248.2009.01351.x.

Liu, W., Jiang, L., Yang, S., Wang, Z., Tian, R., Peng, Z., Chen, Y., Zhang, X., Kuang, J., Ling, N., Wang, S., Liu, L., 2020. Critical transition of soil bacterial diversity and composition triggered by nitrogen enrichment. Ecology 101. https://doi.org/10.1002/ecy.3053.

Liu, X., Zhang, Y., Han, W., Tang, A., Shen, J., Cui, Z., Vitousek, P., Erisman, J.W., Goulding, K., Christie, P., Fangmeier, A., Zhang, F., 2013. Enhanced nitrogen deposition over China. Nature 494 (7438), 459–462. https://doi.org/10.1038/nature11917.

Ma, Q., Wen, Y., Wang, D., Sun, X., Hill, P.W., Macdonald, A., Chadwick, D.R., Wu, L., Jones, D.L., 2020. Farmyard manure applications stimulate soil carbon and nitrogen cycling by boosting microbial biomass rather than changing its community composition. Soil Biology and Biochemistry 144, 107760. https://doi.org/10.1016/j.soilbio.2020.107760.

Macreadie, P.I., Costa, M.D.P., Atwood, T.B., Friess, D.A., Kelleway, J.J., Kennedy, H., Lovelock, C.E., Serrano, O., Duarte, C.M., 2021. Blue carbon as a natural climate solution. Nature Reviews Earth & Environment 2, 826–839. https://doi.org/10.1038/s43017-021-00224-1.

Meng, C., Tian, D., Zeng, H., Li, Z., Yi, C., Niu, S., 2019. Global soil acidification impacts on belowground processes. Environmental Research Letters 14. https://doi.org/10.1088/1748-9326/ab239c.

Millennium Ecosystem Assessment, 2005. Ecosystems and Human Well-Being: Wetlands and Water Synthesis. World Resour. Inst., Washington,D. C.

Min, K., Kang, H., Lee, D., 2011. Effects of ammonium and nitrate additions on carbon mineralization in wetland soils. Soil Biology and Biochemistry 43, 2461–2469. https://doi.org/10.1016/j.soilbio.2011.08.019.

Mo, J., Zhang, W., Zhu, W., Gundersn, P., Fang, Y., Li, D., Wang, H., 2008. Nitrogen addition reduces soil respiration in a mature tropical forest in southern China. Global Change Biology 14, 403–412. https://doi.org/10.1111/j.1365-2486.2007.01503.x.

Mori, H., Maruyama, F., Kato, H., Toyoda, A., Dozono, A., Ohtsubo, Y., Nagata, Y., Fujiyama, A., Tsuda, M., Kurokawa, K., 2014. Design and experimental application of a novel non-degenerate universal primer set that amplifies prokaryotic 16S rRNA genes with a low possibility to amplify eukaryotic rRNA genes. DNA Research 21, 217–227. https://doi.org/10.1093/dnares/dst052.

Piao, S., Wang, X., Park, T., 2020. Characteristics, drivers and feedbacks of global greening. Nature Reviews Earth & Environment 1, 14–27. https://doi.org/10.1038/s43017-019-0001-x.

Pregitzer, K.S., Burton, A.J., Zak, D.R., Talhelm, A.F., 2008. Simulated chronic nitrogen deposition increases carbon storage in Northern Temperate forests. Global Change Biology 14, 142–153. https://doi.org/10.1111/j.1365-2486.2007.01465.x.

Qu, W., Li, J., Han, G., Wu, H., Song, W., Zhang, X., 2019. Effect of salinity on the decomposition of soil organic carbon in a tidal wetland. Journal of Soils and Sediments 19, 609–617. https://doi.org/10.1007/s11368-018-2096-y.

Rosseel, Y., 2012. Lavaan : an R package for structural equation modeling. Journal of Statistical Software 48, 1–93. https://doi.org/10.18637/jss.v048.i02.

Shaygan, M., Baumgartl, T., Arnold, S., Reading, L.P., 2018. The effect of soil physical amendments on reclamation of a saline-sodic soil: simulation of salt leaching using HYDRUS-1D. Soil Research 56, 829–845.

Sun, B., Yan, L., Jiang, M., Li, X., Han, G., Xia, J., 2020. Reduced magnitude and shifted seasonality of CO2 sink by experimental warming in a coastal wetland. Ecology 102, e03236. https://doi.org/10.1002/ecy.3236.

Tao, B., Liu, C., Zhang, B., Dong, J., 2018. Effects of inorganic and organic nitrogen additions on CO_2 emissions in the coastal wetlands of the Yellow River Delta, China. Atmospheric Environment 185, 159–167. https://doi.org/10.1016/j.atmosenv.2018.05.009.

Tian, D., Niu, S., 2015. A global analysis of soil acidification caused by nitrogen addition. Environmental Research Letters 10. https://doi.org/10.1088/1748-9326/10/2/024019.

Wang, F., Sanders, C.J., Santos, I.R., Tang, J., Schuerch, M., Kirwan, M.L., Kopp, R.E., Zhu, K., Li, X., Yuan, J., Liu, W., Li, Z., 2021. Global blue carbon accumulation in tidal wetlands increases with climate change. National Science Review 8. https://doi.org/10.1093/nsr/nwaa296.

Wang, J., Fu, X., Zhang, Z., Li, M., Cao, H., Zhou, X., Ni, H., 2019. Responses of soil respiration to nitrogen addition in the Sanjiang Plain wetland, northeastern China. PLoS One 14 (1), e0211456. https://doi.org/10.1371/journal.pone.0211456.

Wang, H., Liu, S., Zhang, X., Mao, Q., Li, X., You, Y., Wang, J., Zheng, M., Zhang, W., Lu, X., Mo, J., 2018. Nitrogen addition reduces soil bacterial richness, while phosphorus addition alters community composition in an old-growth N-rich tropical forest in southern China. Soil Biology and Biochemistry 127, 22–30. https://doi.org/10.1016/j.soilbio.2018.08.022.

Wilcots, M.E., Schroeder, K.M., DeLancey, L.C., Kjaer, S.J., Hobbie, S.E., Seabloom, E.W., Borer, E.T., 2022. Realistic rates of nitrogen addition increase carbon flux rates but do not change soil carbon stocks in a temperate grassland. Global Change Biology 1–13. https://doi.org/10.1111/gcb.16272.

Wolters, M.L., Sun, Z., Huang, C., Kuenzer, C., 2016. Environmental awareness and vulnerability in the Yellow River Delta: results based on a comprehensive household survey. Ocean & Coastal Management 120, 1–10. https://doi.org/10.1016/j.ocecoaman.2015.11.009.

Wong, K.K., 2013. Partial least squares structural equation modeling (PLS-SEM) techniques using SmartPLS. Marketing Bulletin 24, 1–32.

Xia, J., Wan, S., 2008. Global response patterns of terrestrial plant species to nitrogen addition. New Phytologist 179, 428–439. https://doi.org/10.1111/j.1469-8137.2008.02488.x.

Xu, N., Tan, G., Wang, H., Gai, X., 2016. Effect of biochar additions to soil on nitrogen leaching, microbial biomass and bacterial community structure. European Journal of Soil Biology 74, 1–8. https://doi.org/10.1016/j.ejsobi.2016.02.004.

Zak, D.R., Holmes, W.E., Burton, A.J., Pregitzer, K.S., Talhelm, A.F., 2008. Simulated atmospheric NO_3 deposition increases soil organic matter by slowing decomposition. Ecological Applications 18, 2016–2027. https://doi.org/10.1890/07-1743.1.

Zhang, C., Niu, D., Hall, S.J., Wen, H., Li, X., Fu, H., Wan, C., Elser, J.J., 2014. Effects of simulated nitrogen deposition on soil respiration components and their temperature sensitivities in a semiarid grassland. Soil Biology and Biochemistry 75, 113–123. https://doi.org/10.1016/j.soilbio.2014.04.013.

Zhu, Z., Piao, S., Myneni, R.B., Huang, M., Zeng, Z., Canadell, J.G., Ciais, P., Sitch, S., Friedlingstein, P., Arneth, A., Cao, C., Cheng, L., Kato, E., Koven, C., Li, Y., Lian, X., Liu, Y., Liu, R., Mao, J., Pan, Y., Peng, S., Peuelas, J., Poulter, B., Pugh, T.A.M., Stocker, B.D., Viovy, N., Wang, X., Wang, Y., Xiao, Z., Yang, H., Zaehle, S., Zeng, N., 2016. Greening of the earth and its drivers. Nature Climate Change 6, 791–795. https://doi.org/10.1038/nclimate3004.